New Measurement Results for the Localization of UHF RFID Transponders Using an Angle of Arrival (AoA) Approach

Salah Azzouzi, Markus Cremer, Uwe Dettmar, Rainer Kronberger,
and Thomas Knie
Department of Telecommunication
Cologne University of Applied Sciences, Germany
Email: uwe.dettmar@fh-koeln.de

***Abstract*—In this paper we present new measurement results for an Angle of Arrival (AoA) approach to localize RFID tags at 868 MHz. Self-designed three element antenna arrays, off-the-shelf IDS R901G RFID reader ICs, and UPM Raflatec DogBone RFID tags are used to generate and detect ISO 18000-6C compliant signals. The experimental setup comprises three antenna arrays and a test environment of size 3 times 3 square meters with 25 test points. The AoA is estimated using the phase differences in the complex baseband signals of adjacent antenna elements within one array. A mean positioning error of 0.21 m was achieved for the considered test grid.**

I. Introduction

Nowadays, the identification of objects tagged with RFID transponders is a well established technology. A widespread deployment is underway.
With the introduction of low-cost passive UHF RFID transponders in the UHF frequency band (868 or 915 MHz) the operational range of RFID transponders was enlarged to distances of up to 10 meters. Typical applications include baggage handling, supply chain applications, or fixed asset tracking. However, the full potential of these transponders will be exploited if methods for accurate localization of RFID tagged objects are developed and implemented in addition to the identification feature. A wide range of new applications, amongst others the support of location based services [1], could be opened up by this.

During the last years different approaches to solve the problem of a radio based indoor localization were described in the literature (see e.g. [2]–[6]). All RFID based techniques use measurements between RFID transponders and reader devices and in addition some form of side information about the location of specific readers and/or reference transponders or statistical knowledge about the distribution of RSS values. Measurements are for the Received Signal Strength (RSS), the Angle of Arrival (AoA), the Time of Arrival (ToA), or the Time Difference of Arrival (TDoA). Of course, hybrid procedures are proposed, too (e.g. see [7]–[9]).
For the radio based RFID transponder localization in an indoor environment the time based approaches ToA and TDoA are not appropriate. Both of them require accurate time measurements. However, such measurements are quite difficult to implement with RFID systems since the defined data rates are far too low to receive a sufficient resolution.
The RSS based trilateration methods show to be strongly related to the quality of the propagation channel which again is very sensitive to fading/multipath effects. Due to this an AoA based approach is favored as most promising [10].

In this paper we consider an AoA based localization approach that uses UHF RFID transponders according to the ISO standard 18000-6C (see [11], [12]) and three directional antenna arrays. The theoretical analysis of such systems in typically time variant multipath environments is rather complicated and often relates to simplified signal models (e.g. [13], [14]). This again results in significant differences between simulation and measurement results [6]. Due to the difficulty to access the IQ signals from a commercial RFID reader needed to evaluate the phase differences for AoA based approaches up to now most authors restrict to system simulations or the use of non standard compliant hardware. [15]–[17]
The focus of this work is the evaluation of the achievable accuracy for a transponder localization under real life conditions. A simple RFID based localization approach using *off-the-shelf* components. A setup using IDS R901G RFID Reader ICs, UPM Raflatec DogBone RFID transponders and multiple self-designed three element antenna arrays will be considered. The test environment is a seminar room in which a RFID transponder is placed at 25 different grid positions of a square plane of size 3 times 3 meters. The position of the transponder is then determined for each position by estimating the angle of arrival measured by three antenna arrays placed outside of the plane.
The described setup fits to many different practical scenarios including the problem of finding RFID tagged books on a desk for sorting purposes in a library or the localization of tools or work pieces on a table during the fabrication process.
The rest of the paper is organized as follows. Section II describes the AoA based approach to estimate the position of an object under investigation. The experimental setup and measurement results are presented in sections III and IV. Section V concludes the paper with a summary and discussion.

978-1-4244-9606-8/11/$26.00 ©2011 IEEE

II. Angle of Arrival (AoA) based localization approach

The standard AoA approach for the localization of a RFID transponder consists of two steps: In the first step the incidence angles Θ_n of the backscattered transponder signal with respect to known positions of N receive antennas are estimated. In the second step the position of the transponder is determined based on the knowledge of the angles Θ_n by using a triangulation approach.

To achieve the direction finding principle different approaches are possible. The main AoA can be determined by scanning the azimuth plane with the main directive lobe of the receiving antenna. This can be done either mechanically by turning the antenna (conventional radar principle) or in a more sophisticated way by turning the antenna beam electronically using the phased array antenna principle. Basically, a phased array is composed of M individual antenna elements, which are distributed and oriented in a linear or two dimensional configuration. The phase (and amplitude) of the received tag signal from each antenna element is controlled to adjust the angle of the antenna beam. The antenna network contains the required M phase shifters (see Fig.1 b) Then only one conventional RFID receiver is necessary. Information of the direction towards the tag results from the different phase angles of the array. This simple principle has been in widespread use a lot in communications for many years. The main disadvantage lies in the realization of small and compact phase shifters for 868 MHz. To overcome this, the digital beam forming principle [18] can be applied as well. Instead of using one single RFID receiver, M down converters are required. Each path provides the digital IQ information from each antenna element (see Fig.1 a). Then, extended processing allows the determination of the AoA with well known techniques.

Consider a linear antenna array of M antenna elements arranged along a line as depicted in Fig.2. The distance d between adjacent elements is assumed to be fixed resulting in a constant phase shift of $\Delta\phi$ between received signals of adjacent antenna elements. $\Delta\phi$ is related to the incidence angle Θ of a plane wave, measured with respect to the normal to the linear array as

$$\Delta\phi = \frac{2\pi d}{\lambda} \sin\Theta.$$

λ is the carrier wave length [19].

To estimate the incidence angle Θ the received signals from the M antenna elements are weighted and combined in a way to satisfy a specified quality criteria like e.g. maximizing the total received power [20].

In case of a $M = 2$ element array the estimation of the AoA can be simplified by evaluating the phase difference between the complex received signals at the two antenna elements [20], [21]. Applying the root-MUSIC method (see e.g. [14], [16]) Θ is calculated as

$$\hat{\Theta} = \arcsin\left(\frac{\lambda}{2\pi d}\Delta\hat{\phi}\right) \quad (1)$$

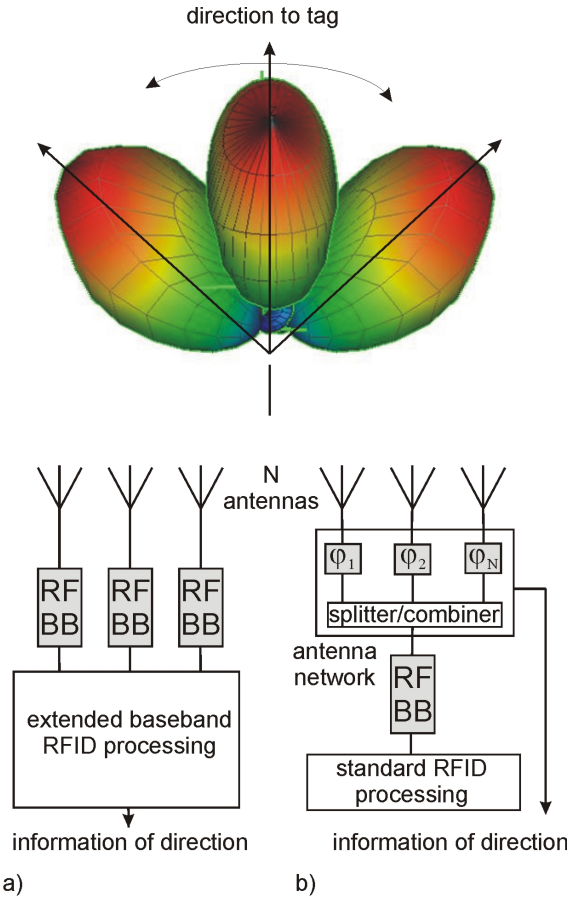

Fig. 1. Direction finding concepts with phased array a) and digital beamforming b) or analogue phase shifters

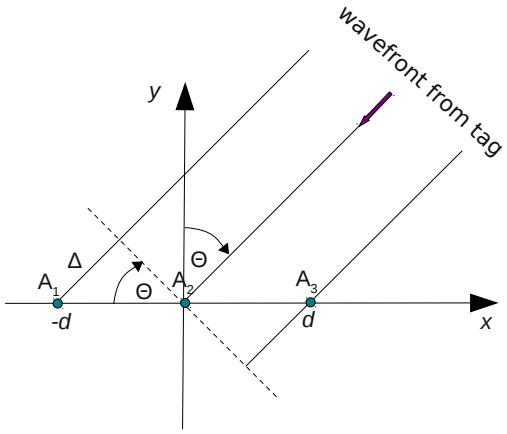

Fig. 2. Linear antenna array with $M = 3$ elements

where

$$\Delta\hat{\phi} = \angle\{E[x_1^*(t)x_2(t)]\}. \quad (2)$$

* denotes the complex conjugate, $E[.]$ the statistic expectation value, and $\angle\{.\}$ is the phase of a complex variable. $x_1(t)$ and $x_2(t)$ describe the two IQ demodulated and filtered complex baseband signals from antenna 1 and 2, respectively. In general $d < \lambda/2$ is chosen to avoid the appearance of grating lobes.

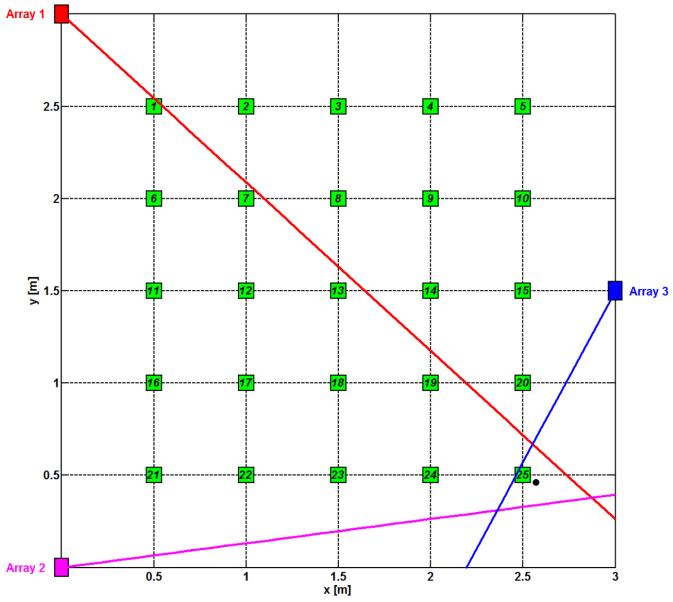

Fig. 3. Grid for the localization measurements

Having estimated the angles of incidence $(\Theta_1, ...\Theta_N)$ for all N antenna arrays in the second step the probability of the transponder being in position (x, y) under observation of $(\Theta_1, ...\Theta_N)$

$$Pr((x, y)|(\Theta_1, ...\Theta_N))$$

has to be maximized. Assuming perfect knowledge of the incidence angles $(\Theta_1, ...\Theta_N)$ this can be done by constructing lines from the N antenna positions towards the direction of the corresponding Θ_n. One interception point results representing the position of the transponder. In this case even a setup with only two arrays is sufficient to exactly find the position of the object under investigation. However, in reality imperfections in measuring the exact angle and perturbations like reflections or multipath lead to substantial deviations between estimated and correct position.

Consider the setup with three antenna arrays at defined positions (x_i, y_i) with $i = 1, 2, 3$ depicted in Fig.3. The lines initiating from the antenna arrays mark the directions of the transponder based on the estimated angles Θ_1, Θ_2 and Θ_3. In general, these lines form a triangular intersection plane with the vertices given by the intersection points instead of only one single point. The quality of estimation of the transponder position depends on the choice of the intersection point. Thus including the measurements from more than two receive antennas may lead to a better performance and can be especially useful in highly deterministic short range multipath environments as characterized in [21].

Two strategies were followed to determine the transponder position in our setup with three antenna arrays: In the first approach the centroid of the triangle defined by the three intercept points was used as estimate for the actual transponder position. If a uniform distribution of the correct transponder position within the triangle is assumed the centroid minimizes the mean square error $E\{(\mathbf{x}_t - \mathbf{x}_e)^2\}$ where $\mathbf{x}_t$ is the actual position and $\mathbf{x}_e$ is the estimated position of the RFID transponder.

In the second approach a subset of two out of three arrays is chosen to calculate the position of the transponder for each test point. The intercept point of the lines initiating from these two antennas is used as the estimate for the transponder position. The subset is determined as a function of the estimated angle $\hat{\Theta}_3$ of antenna 3 as follows:
If $\hat{\Theta}_3 \geq 0$ choose the intercept point of arrays 1 and 3 else choose the intercept point of arrays 2 and 3
This strategy is based on the observation that the quality of the estimation is usually bad, if the measurement point is close to a line connecting two antenna locations and on the results for the approximation of the localization error from [14].

III. Experimental Setup

A. RFID Localization System

The system has been realized with three element phased arrays. Three similar RFID receivers were built for the down conversion of the signals. As the main information of the direction is derived from the IQ signals, all receivers are synchronized in phase by one reference signal (see Fig.6). For the localization system three similar antenna arrays were built up and positioned at two corners and the middle of the opposite side (see Fig.3). The IQ signals from each antenna element are sampled and read out by a microcontroller for further processing. The estimates for Θ_n of the three arrays are calculated according to equations 1 and 2 and used to compute and plot the estimated position of the transponder. This is done on a host computer connected to the microcontrollers.
The estimate for the angle of incidence Θ_n at array n is derived as the mean value $\Theta_n = (\Theta_n^{(1,2)} + \Theta_n^{(2,3)})/2$ of the estimate $\Theta_n^{(1,2)}$ of antenna elements 1 and 2 and $\Theta_n^{(2,3)}$ the estimate of elements 2 and 3. Element 2 is the center element of the $n-$th array.

For the calculation of the AoA the transponder response containing the Electronic Product Code and the CRC of length 16 is evaluated. From this signal 250 samples (relating to around 70 symbols) are used for computing the correlation as given by equation 2. From the estimate $\hat{\Delta\phi}$ the spatial angle $\hat{\Theta}$ is calculated. As described in [16] the phase characteristic of the antenna pattern distorts the determination of the spatial angle $\hat{\Theta}$. To eliminate this effect a reference measurement of the characteristic $\Theta = f(\hat{\Theta})$ was conducted in an anechoic antenna chamber. This characteristic was used in the sequel to correct $\hat{\Theta}$.

B. Antenna

The antennas are designed as microstrip patch antenna arrays with three vertically polarized elements in a horizontal line. Each single element provides a beam width of approximately 55 deg and has a size of 79 $\times$ 50 mm. The overall size of the array is 290 mm $\times$ 200 mm. The distance between adjacent antenna elements is $d = 11.5\,\mathrm{cm}$ leading to $d/\lambda \approx 0.3$. Simulations and measurements have shown, that a

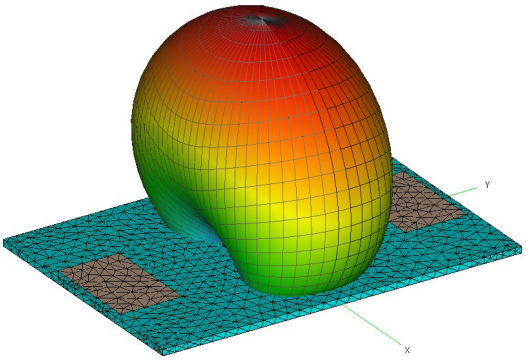

Fig. 4. Simulated 3D antenna diagram

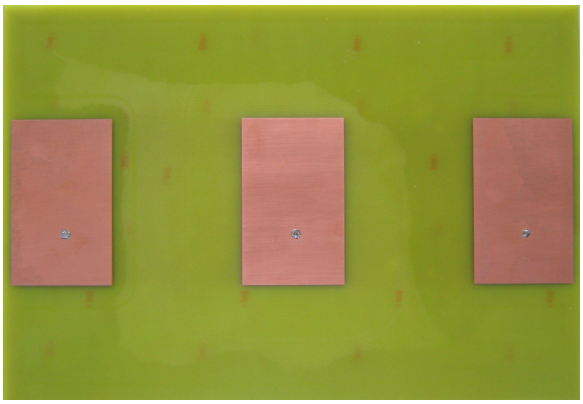

Fig. 5. Realized three element antenna array

beam steering angle of approximately $\pm 60°$ can be achieved with the array. The overall gain of the antenna in the main direction is approximately 6.5 dBi and still 4.5 dBi towards $\pm 60°$ (see Fig.4).

The whole array is realized on a FR4 substrate as shown in Fig.5.

C. Signal processing hardware

Fig.6 shows the block diagram of the signal processing hardware that was used to communicate with the RFID tag and to sample the I and Q samples needed for the calculation of the AoA. Each of the modules was built on a separate circuit board attached to a common base board used for power supply and signal distribution (see Fig.7). The antenna array introduced in section III-B is connected to three RFID reader modules. The antenna element in the middle of the array and the reader module attached to it can be used to communicate with the RFID tag and to read the Electronic Product Code (EPC) stored on every ISO18000-6C compliant tag. During this reading process the two other reader modules connected to the two patch elements at both sides of the antenna array are switched to a listening mode. The main component of each of the reader modules is the integrated ISO18000-6C RFID reader IC R901G developed by IDS Microchip. In addition to the complete analog and digital signal processing parts for

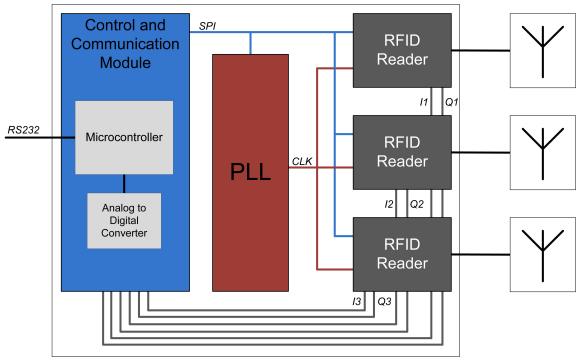

Fig. 6. Block diagram of the signal processing hardware

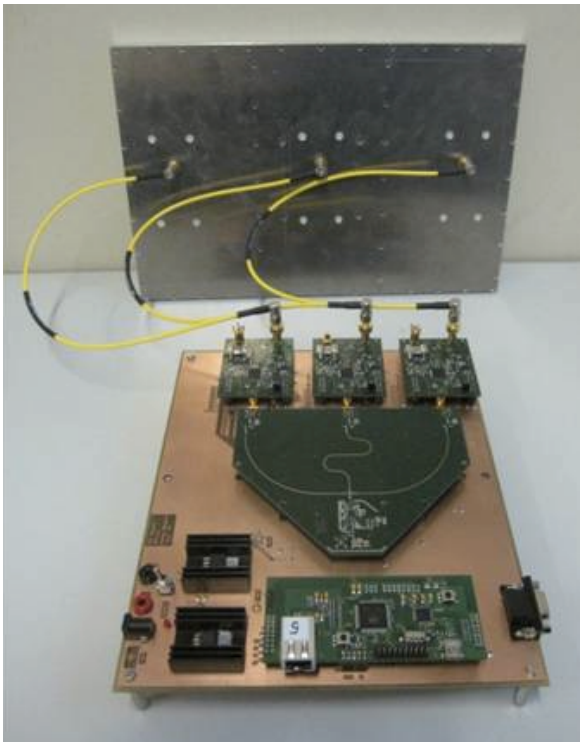

Fig. 7. Signal processing hardware and antenna array

modulation, demodulation and data encoding/decoding this IC includes two analog mixers providing the baseband I and Q parts of the received tag signal. The R901G can be controlled and configured via serial (SPI) or parallel interface. It operates in the frequency range between 860 MHz and 960 MHz.

The PLL module is used to feed every RFID reader module with a synchronous 868 MHz clock signal. The integral part of that module is the ADF4360-7 IC by Analog Devices. This integrated synthesizer and VCO can be configured and controlled via SPI interface. It supports a frequency range between 350 MHz and 1800 MHz. The synchronous clock is used as a reference signal for the phase difference measurement in the calculation of the AoA.

The control and communication module comprises of a microcontroller (ATMEL AT91SAM7X256 with 32 bit ARM7

core) and an analogue to digital converter (Maxim MAX1304). The microcontroller configures and controls the PLL module and the three RFID reader modules using two integrated SPI interfaces. This module additionally executes every step in the ISO18000-6C communication protocol that is needed to read the tag's EPC. After reception of the EPC the analog signals from each of the antenna array elements are mixed down to the base band and distributed to the analog to digital converter on the control and communication module. The ADC simultaneously samples all six baseband signals (I1-I3 and Q1-Q3, see Fig.6) with a maximum sampling rate of 680 ksps and a 12 bit resolution for each signal. Data is exchanged with the microcontroller using a 12-bit parallel interface.

To send the values of the sampled analog signals to the PC for further analysis the microcontroller's UART interface is used. In combination with a level shifter for RS232 the signal processing hardware is able to communicate with a PC software via serial port interface.

D. Measurement environment

The measurements were conducted in a test grid of size 3.0 m $\times$ 3.0 m comprising of 25 measurement points with a distance of 0.5 m in x direction and 0.5 m in y direction to each other (see Fig.3). The grid was set up in a standard 7.5 m $\times$ 12 m seminar room. Three sides of the room were bounded by stone walls and the other side by a stone wall with windows and three radiators. A standard passive ISO 18000-6C DogBone RFID transponder by UPM Raflatac was used for measurement purposes. It stores a 96-bit EPC and is optimized for corrugated and plastic materials. It is mainly employed in industrial environments for supply chain management. For the localization process the tag was attached to a piece of corrugated board and put on a 1.5 m stand above the floor.
The signal processing hardware and the antenna array were put on a table 1.5 m above the floor. To avoid the need for a directional coupler a separate low gain transmit antenna was employed during the measurements. It was placed on a 1.5 m high stand. The transmit power was 2W ERP (3,28 W EIRP). The antenna arrays were positioned in two corners and the middle of one side of the plane (see Fig.3). For each antenna array the angles of arrival of the tag positioned at the 25 measurement points were calculated on a host PC. for this purpose the PC initiated the EPC reading process and received the sampled values of the I and Q components of the tag signal received by each of the array elements.

IV. Experimental results

A. Quality of the measurements for the AoA

To test the quality of the angle estimation a measurement with one antenna array in a nearly free space environment (balcony on the 8th floor of the university) was conducted. Similar to the description in [20] a UPM Raflatec DogBone transponder was moved by means of a nylon cord on a straight line in front of an array in a range $-45° < \Theta < 45°$. The shortest distance (at $\Theta = 0°$) between tag and antenna array was $d_0 = 2,5\,\mathrm{m}$. An angle measurement was performed for

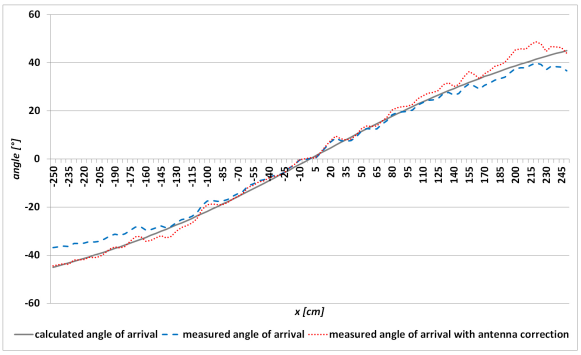

Fig. 8. Measurement results for one three element antenna array

TABLE I
Mean values for approach 1

$m_X = E\{\Delta X\}$	0.18 m
$m_Y = E\{\Delta Y\}$	0.17 m
$m_D = E\{\Delta D\}$	0.26 m
$\sigma_X^2 = E\{(\Delta X - m_X)^2\}$	0.05 m^2
$\sigma_Y^2 = E\{(\Delta Y - m_Y)^2\}$	0.02 m^2
$\sigma_D^2 = E\{(\Delta D - m_D)^2\}$	0.06 m^2

$N = 100$ positions along the line equally spaced in 0.05 m distance. The results of these measurements are depicted in Fig.8 The figure shows the theoretical curve, one curve without any correction of the antenna phase characteristic, and the curve where the measured phase is corrected by the measurement results of the phase characteristic of the antenna array achieved in the anechoic chamber. The root of the averaged squared error

$$\epsilon = \sqrt{\frac{1}{N+1}\sum_{i=0}^{N}(\hat{\Theta}_i - \Theta_i)^2} \tag{3}$$

was computed. $\hat{\Theta}_i$ denotes the measured angle of the transponder, Θ_i is the actual angle figured from the geometry of the setup. For the uncorrected curve $\epsilon = 3.41°$. The corrected curve leads to $\epsilon = 2.39°$. Restricting the measurement range to $-33.5° < \Theta < 18.1°$ as in [20] one gets $\epsilon = 2.12°$ for the uncorrected and $\epsilon = 1.65°$. for the corrected curve.

B. Measurement results for the transponder localization

The measurement results in the $3\,\mathrm{m} \times 3\,\mathrm{m}$ measurement grid are shown in Fig.9 for both approaches. The upper numbers at each measurement point show the absolute value of the localization error (in meters) for the first approach (i.e. choose the centroid of the triangle defined by the three intercept points as transponder position), the lower numbers those for the second approach (i.e. preselection of two antennas).

Table I shows the mean values for the first approach. The estimated position of the transponder (X_e, Y_e) and the deviation $(\Delta X, \Delta Y) = (|X_e - X_t|, |Y_e - Y_t|)$ from the exact position were calculated for all valid test positions. The position estimation failed for three test points since the

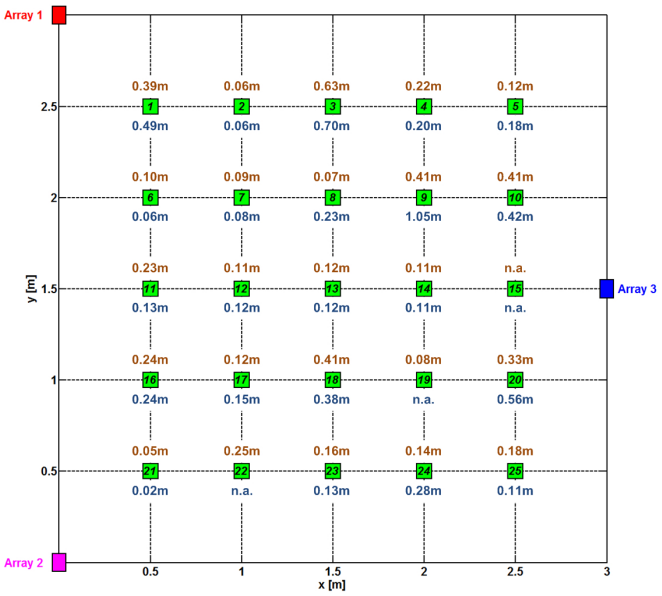

Fig. 9. Localization results for both approaches

TABLE II
MEAN VALUES FOR APPROACH 2

$m_X = E\{\Delta X\}$	0.14 m
$m_Y = E\{\Delta Y\}$	0.13 m
$m_D = E\{\Delta D\}$	0.21 m
$\sigma_X^2 = E\{(\Delta X - m_X)^2\}$	0.02 m^2
$\sigma_Y^2 = E\{(\Delta Y - m_Y)^2\}$	0.01 m^2
$\sigma_D^2 = E\{(\Delta D - m_D)^2\}$	0.02 m^2

computed positions lay outside the test grid. These points were ignored in the computation of the mean values. The distance between correct and estimated position of the transponder can be determined easily from ΔX and ΔY as

$$\Delta D = \sqrt{(\Delta X)^2 + (\Delta Y)^2} \tag{4}$$

The mean values m_X, m_Y and m_D as well as the variances σ_X^2, σ_Y^2 and σ_D^2 are shown in in table I.

Consider in more detail the results for test point 25 as shown in Fig.3. The black dot inside the triangle represents the centroid as the estimated position. It can be observed that the inaccuracy of the measurement at antenna 1 is partly compensated by the measurements of the two other antennas. Thus the centroid of the intersection plane gives a better result than the interception points.

Mean values for the performance of the second approach are shown in table II. For this approach the localization failed only at one test point. For the considered test environment with 25 positions, the second approach leads to better results.

Perturbations originate from propagation effects like attenuation or multi path and from tolerances in the measurements of the direction of arrival due to the radiation pattern of the antennas. It shows that reflections from obstacles in the direct vicinity of the test environment affect the quality of the estimation. Most measurement points with a large deviation between actual and estimated position were clustered at the borders of the test environment. This underlines the influence of reflections on the quality of the localization approach.

V. Conclusions and Outlook

In this paper the localization of UHF RFID transponders using an AoA approach was investigated by conducting a measurement campaign with off-the-shelf components for generation and processing of ISO 18000-6C compliant signals. The phase difference between pairs of antenna elements in each antenna array was used to estimate the angle of arrival. By a combination of the estimates from three antenna arrays the position of the transponder was calculated for 25 test points. The results of the measurements are quite promising and show that a rather accurate estimation of the transponder locations is possible even in typical office environments. For a grid of size 3×3 meters with 25 test locations the mean deviation figures out to be $E\{\Delta D\} = 0.21\,\text{m}$ with a standard deviation of $\sigma_{\Delta D} = 0.13\,\text{m}$. To cope with the distortion of the measurement results by the phase characteristic of the antenna array a reference measurement to determine the characteristic $\hat{\Theta} = f(\Delta\hat{\phi})$ was conducted in an anechoic antenna chamber. The resulting function was later on used to correct the measurement results.

The results confirm that localization by AoA estimation is a practically feasible approach for the above mentioned scenarios. Most of the bad measurement results were clustered at the borders of the test environment which is due to multi path. However, distortions due to multi path did not affect the measurement results too strongly. No reflecting objects were present within the test grid and only few in its vicinity.

Power control and the beam forming capability of the antenna arrays can be exploited to combat the influence of multi path interference on the quality of the localization. Single strong distorting signals from specific directions could be nulled. In case of more than two measuring antenna arrays multiple estimates from subsets of the antenna measurements can be evaluated and combined. Unreliable measurements can be excluded, e.g., by investigating corresponding RSS values.

Another approach can combine one omni directional receive antenna with multiple electronically steerable directive antenna arrays for transmission. By varying the transmit power one can exploit the very sensitive response threshold of the RFID transponders to refine the quality of the angular measurement. At minimum transmit power the transponder will only respond if the transmit antenna beam points directly at the transponder.

Acknowledgment

This work was partially sponsored by the German Federal Ministry of Education and Research.

References

[1] D. Hähnel, W. Burgard, D. Fox, K. Fishkin, and M. Philipose, "Mapping and localization with RFID technology," Intel Research, Tech. Rep., 2003. [Online]. Available: seattleweb.intel-research.net/people/matthai/pubs/icra04.pdf

[2] Q. Spencer, M. Rice, B. Jeffs, and M. Jensen, "A statistical model for angle of arrival in indoor multipath propagation," in *IEEE Vehicular Technology Conference*, 1997, pp. 1415–1419.

[3] Chon, Jun, Jun, and An, "Using RFID for accurate positioning," in *International Symposium on GNSS/GPS*, Sydney, Australia, Dec. 2004.

[4] Localization using direction of arrival. Frauenhofer Institut für integrierte Schaltungen. [Online]. Available: www.iis.fraunhofer.de/fhg/iis/EN/bf/ec/nl/omf/lw/index.jsp

[5] H. Tatsumi, Y. Murai, T. Araki, and M. Miyakawa, "Rfid localization for the visually impaired," *Automation Congress, 2008. WAC 2008. World*, pp. 1 – 6, 2008. [Online]. Available: http://ieeexplore.ieee.org/xpl/freeabs_all.jsp?arnumber=4698957

[6] C. Hekimian-Williams, B. Grant, X. Liu *et al.*, "Accurate localization of rfid tags using phase difference," in *Proceedings of the RFID 2010*. IEEE, April 2010.

[7] M. Bouet and A. L. Dos Santos, "Rfid tags: Positioning principles and localization techniques," *2008 1st IFIP Wireless Days*, pp. 1–5, 2008. [Online]. Available: http://ieeexplore.ieee.org/lpdocs/epic03/wrapper.htm?arnumber=4812905

[8] C. Byoung-Suk, L. Joon-Woo, and L. Ju-Jang, "An improved localization system with rfid technology for a mobile robot," *Industrial Electronics, 2008. IECON 2008. 34th Annual Conference of IEEE*, pp. 3409 – 3413, 2008. [Online]. Available: http://ieeexplore.ieee.org/xpl/freeabs_all.jsp?arnumber=4758508

[9] G. Chandrasekaran, M. A. Ergin, J. Yang *et al.*, "Empirical evaluation of the limits on localization using signal strength," *2009 6th Annual IEEE Communications Society Conference on Sensor, Mesh and Ad Hoc Communications and Networks*, pp. 1–9, 2009.

[10] N. Patwari, J. Ash, and S. Kyperountas, "Locating the nodes," *IEEE Signal Processing Magazine*, no. 54, July 2005.

[11] *ISO/IEC 18000-6:2004 Information technology – Radio frequency identification for item management - Part 6: Parameters for air interface communications at 860 to 960 MHz*, ISO/IEC Std., 2004.

[12] *EPC Radio-Frequency Identity Protocols Class-1 Generation-2 UHF RFID Protocol for Communications at 860 MHz – 960 MHz*, EPC global Std., Rev. 1.0.9, January 2005.

[13] M. J. Abedin and A. S. Mohan, "Rfid localization using planar antenna arrays with arbitrary geometry," *2008 Asia-Pacific Microwave Conference*, pp. 1–4, 2008. [Online]. Available: http://ieeexplore.ieee.org/lpdocs/epic03/wrapper.htm?arnumber=4958395

[14] Y. Zhang, M. B. Amin, and S. Kaushik, "Localisation and tracking of passive rfid tags based on direction estimation," *Internation Journal of Antennas and Propagation*, vol. Volume 2007, no. ID 17426, 2007.

[15] A. Alma'aitah, K. Ali *et al.*, "3d passive tag localization schemes for indoor rfid applications," in *ICC 2010*, Mai 2010.

[16] J. Wang, M. B. Amin, and Y. Zhang, "Signal and array processing techniques for rfid readers," in *Wireless Sensing and Processing*, ser. Proc. of SPIE, vol. 6248, 2006.

[17] M. Abedin and A. Mohan, "Use of smart antennas for the localisation of rfid reader," in *APMC 2009*, Dec. 2009.

[18] R. Hansen, *Phased Array Antennas*. New York: John Wiley & Sons, 1998.

[19] S. Haykin, *Adaptive Filter Theory*. Upper Saddle River, New Jersey: Prentice-Hall, 1996.

[20] C. Angerer, R. Langwieser, and M. Rupp, "Direction of arrival estimation by phased arrays in rfid," in *Proceedings of the 3rd international EURASIP Workshop on RFID Technilogy*, Lan Manga del Mar Menor, Sep. 2010.

[21] P. V. Nikitin, R. Martinez *et al.*, "Phase based spatial identification of uhf rfid tags,," in *IEEE RFID 2010*, April 2010.